This article has been accepted for publication in a future issue of this journal, but has not been fully edited. Content may change prior to final publication. Citation information: DOI 10.1109/JPHOT.2015.2513199, IEEE Photonics Journal

A Fiber Laser Using Graphene-Integrated 3D Microfiber Coil

Cheng Li, Jin-hui Chen, Shao-cheng Yan, Fei Xu*, and Yan-qing Lu,

National Laboratory of Solid State Microstructures and College of Engineering and Applied Sciences, Nanjing University, Nanjing 210093, China

Abstract: We demonstrate a state variable fiber pulse laser based on a graphene-integrated microfiber device. A 3D microfiber coil integrated with graphene acts as a polarization sensitive saturable absorber. By adjusting the polarization controllers, stable Q-switched pulses and mode-locked rectangular pulses are observed. To our knowledge, this is the first study conducted to achieve switching between rectangular pulses and Q-switched pulses while keeping the pump power constant. The rectangular pulses have a pulse width and repetition rate of ~10 ns and ~940 kHz, respectively, and the Q-switched pulses have a pulse width and repetition rate of ~40 μs and ~4.8 kHz, respectively. (*Email: feixu@nju.edu.cn)

Index Terms: Fiber laser, graphene saturable absorber, Q-switching, rectangular pulse.

1. Introduction

In recent decades, pulse fiber lasers have been extensively investigated because of their wide applications in the fields of medicine, sensing, communication, and materials processing. Different pulses can be produced in various active or passive technologies [1]- [3]. Because of its simple structure, much attention has been given to the passive fiber laser using a semiconductor saturable absorption mirror (SESAM) [4], [5], nonlinear polarization rotation (NPR) technique [6], [7], or saturable absorber (SA) [8]- [10].

After the first demonstration of a graphene SA in 2009, a number of fiber lasers have been manufactured because of graphene's ultrafast response time and gapless energy property [11]- [13]. However, the interaction lengths between graphene and optical fields are limited by the thickness of single layer graphene in fiber lasers. For enhancing the interaction between the optical field and graphene, researchers transfer the graphene on a D-shape fiber [14] or a straight microfiber (MF) [15]. In 2014, Kou et al. proposed a graphene-integrated MF device by wrapping a MF on a graphene-coated rod that can easily achieve sufficient light–graphene interaction and demonstrated the application of broadband polarization manipulation, such as a polarizer and high-Q single-polarization resonator [16]. Owing to the extraordinary saturable absorption of graphene, 3D MF-graphene (MFG) hybrid polarization-based devices have applications that are more promising in a pulse fiber laser system.

Moreover, switching between mode-locked pulses and Q-switched pulses has attracted considerable attention from people who need a compact laser with more functionality. In practice, a fiber laser cavity with SA has been demonstrated to produce Q-switched, Q-switched mode-locked, and mode-locked pulses by using a pump power variation method. However, the pump power, cavity length, and polarization controller (PC) need to be adjusted simultaneously to obtain the stable state [17], [18]. Lin et al. proposed a fiber laser by using a SESAM and polarizer. In their fiber laser systems, switching between different states in the fiber laser is possible just by adjusting the PC [19].

In this paper, we demonstrate a state variable erbium-doped fiber laser (EDFL) by using a MFG which acts as an integrated polarization sensitive SA. On one hand, the interaction between the evanescent field of the MF and graphene can provide sufficient saturable absorption. On the other hand, the cavity is sensitive to the PCs because of the polarization sensitivity of the MFG device. Stable Q-switched and mode-locked pulses can be obtained under a fixed pump power. In addition, the rectangular pulses are observed in our EDFL. The rectangular pulses have a pulse width and repetition rate of ~10 ns and ~940 kHz, respectively; the Q-switched pulses have a pulse width and repetition rate of ~40 μs and ~4.8 kHz, respectively. To our knowledge, this is the first demonstration to achieve switching between mode-locked rectangular pulses and Q-switched pulses while keeping the pump power constant.

This article has been accepted for publication in a future issue of this journal, but has not been fully edited. Content may change prior to final publication. Citation information: DOI 10.1109/JPHOT.2015.2513199, IEEE Photonics Journal

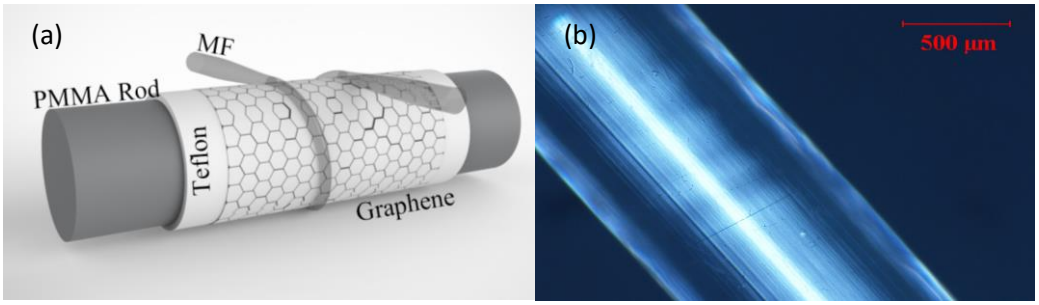

Fig. 1. (a) The schematic and (b) the optical microscope image of the MFG device.

2. MFG fabrication

Fig. 1(a) shows the schematic of the MFG device. The polarization sensitive SA was fabricated by wrapping the MF on the graphene-coated rod. The MF was fabricated by using the flame-drawing technique to stretch single mode fiber (Corning SMF-28) [20]. The diameter and length of the MF used in this study are ~3 μm and ~5 mm, respectively. In order to prepare the graphene-coated rod, a piece of graphene (deposited on the Cu substrate) was immersed in a ferric chloride solution (0.5 mol/L) to corrode the Cu substrate. To prevent the graphene from falling apart in the $FeCl_3$ solution, the polymethyl methacrylate (PMMA) with anisole (~4 wt%) solution was spin coated on the surface of the graphene. Then, a PMMA rod (1 mm diameter) was used as a holder for the graphene without Cu substrate. Next, the rod was immersed into the acetone to remove the PMMA coating on graphene. In order to reduce the loss induced by the relatively high index of the rod (~1.5), Teflon (Teflon AF 601S1-100-6, DuPont, index ~1.3) was dip-coated on the rod surface before transferring the graphene. Finally, the 3 μm-diameter MF was wrapped on the graphene-coated rod with a single coil. Fig. 1(b) shows the optical microscope image of the MFG device. In this transfer method, the PMMA on the graphene cannot be completely removed in some partial ranges, limiting the application of the MFG device in a high power laser system.

It is already known that the MFG device can provide high polarization sensitivity. In the study conducted by Kou, the polarization dependent loss (PDL) of their device could be as high as ~16 dB and the insertion loss (IL) was also as high as 20 dB in 1,550 nm. However, this IL is too large to be used in a fiber laser. In order to decrease the IL, the MF was wrapped in a single coil and a rod of diameter 1 mm was used in this study. The IL of our MFG device was observed to be ~4 dB. It was acceptable by appropriately increasing the length of the gain fibers. The nonlinear absorption of the MFG device in 1,550 nm was measured, as shown in Fig. 2. The modulation depth was estimated to be ~2%.

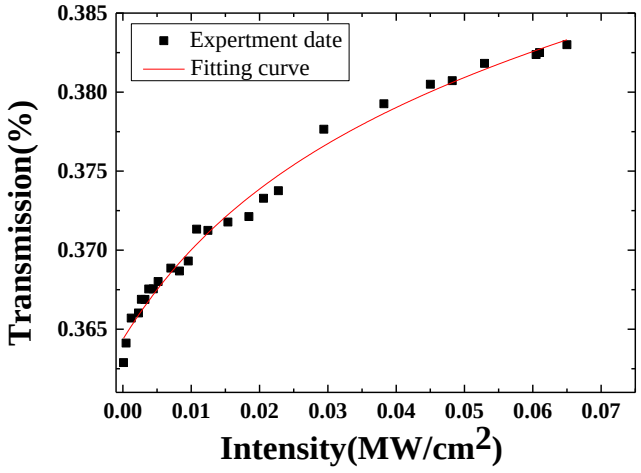

Fig. 2. The nonlinear absorption of the MFG as function of the intensity at 1,550 nm.

This article has been accepted for publication in a future issue of this journal, but has not been fully edited. Content may change prior to final publication. Citation information: DOI 10.1109/JPHOT.2015.2513199, IEEE Photonics Journal

3. EDFL setup

Fig. 3 shows the setup of the fiber laser. It consists of an erbium-doped fiber (~7 m, Nufern EDFC-980-HP C-band, ≥ 3 dB/m absorption at 980 nm, the GVD is ~15.6 ps^2/km at 1550 nm), single-mode fiber (~200 m, Corning SMF-28, the GVD is ~23 ps^2/km), a wavelength division multiplexer to couple the 980 nm pump source to the gain fiber, a polarization insensitivity isolator (PI-ISO) to keep the pulses rounding in one direction, two PCs to adjust the polarization of the pulses, our fabricated MFG device, and a fiber coupler with a 10% output ratio. To avoid the unnecessary reflections, all of above-mentioned components were fusion-spliced by single mode fibers and not using ferrule connector in the cavity. The total length of the cavity was ~220 m. An optical spectrum analyzer (Yokogawa AQ6370C) and a 200 MHz oscilloscope (Agilent InfiniiVision DSO-X 4024A) were used to monitor the pulses.

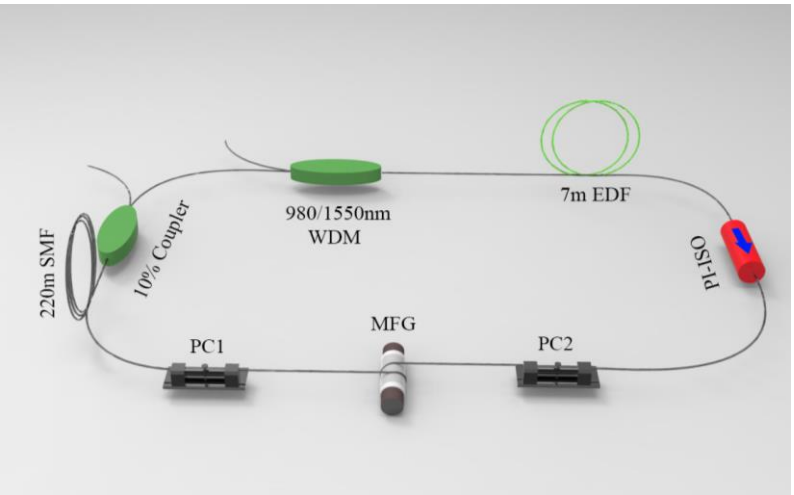

Fig. 3. Experiment setup of the EDFL.

The SA and NPR techniques are employed to our long-cavity fiber ring laser [21]. Under certain approximations, the transmission coefficient of NPR can be expressed as [22], [23]

$$|T|^2 = \sin^2\theta\sin^2\varphi + \cos^2\theta\cos^2\varphi + \frac{1}{2}\sin(2\theta)\sin(2\varphi)\cos(\Delta\phi) \quad (1)$$

where $\Delta\phi = \Delta\phi_{PC} + \Delta\phi_{LB} + \Delta\phi_{NL}$ is the net phase delay between the fast and slow axes of the fiber. $\Delta\phi_{PC}$ is the PC induced phase delay, $\Delta\phi_{NL} = -2\gamma LP\cos(2\theta)/3$ is the fiber induced nonlinear phase change, and $\Delta\phi_{LB} = 2\pi LB_m/\lambda$ is the phase delay caused by the linear fiber birefringence. The polarizer and analyzer have an orientation of angles θ and φ, respectively, with respect to the fast axis of the fiber. When the fiber laser is installed, θ and φ can be regarded as constants. Then, equation (1) can be simplified as

$$|T|^2 \sim \cos(\Delta\phi_{PC} + \Delta\phi_{LB} + \Delta\phi_{NL}) \quad (2)$$

When the light propagates in the cavity, the loss it experiences is strongly dependent on the net phase delay. The cavity can generate a positive feedback, as the actual cavity transmission increases under the effect of the nonlinear polarization rotation. On the contrary, the cavity also can generate a negative feedback if the phase delay meets certain conditions. Our fabricated MFG device had a relatively low PDL

This article has been accepted for publication in a future issue of this journal, but has not been fully edited. Content may change prior to final publication. Citation information: DOI 10.1109/JPHOT.2015.2513199, IEEE Photonics Journal

(~2 dB) for attaining a relatively low IL. By using equation (2), the long SMF was necessary to enhance the NPR effect in our laser system. Meanwhile, the NPR effect was compared to the SA effect in the long cavity; and the states of the laser could be easily switched by adjusting the PCs. When we removed the long SMF, the stable state cannot be observed in our laser.

4. Results

First, the Q-switching operation was achieved by adjusting the two PCs. Fig. 4(a) shows the Q-switched pulses of the fiber laser with the pump power of 72 mW. The repetition rate and pulse width were 4.8 kHz and 40 μs, and the asymmetry of the pulse is somewhat significant. The main reason is that the inversion density at the rise edge is higher than the density at the fall edge, so the attenuation rate is different. A dual-wavelength emission state was realized as shown in Fig. 4(b). The centers of the dual-wavelength were ~1,542.1 nm and ~1,559.5 nm, the linewidth of the Q-switched pulse can be improved by adding a filter in the cavity.

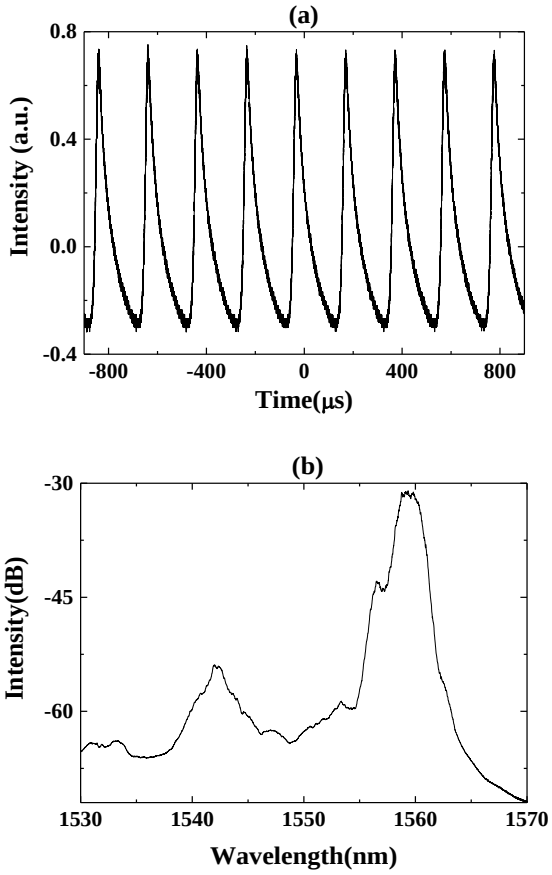

Fig. 4. (a) Q-switched pulses and (b) The spectrum of the Q-switched pulses.

By further adjusting the two PCs, the stable mode-locked pulses were obtained by keeping the pump power constant. The repetition rate of the pulses was ~940 kHz, obtained from Fig. 5(a), which is approximately equal to the repetition rate of the 220 m long cavity (~ 940 kHz). From Fig. 5(b), the 3 dB spectral bandwidth was 1.1 nm, and the center wavelength was ~1,559.5 nm. A series of Kelly sidebands, which could be reduced by dispersion management of the cavity and optimizing the length of the fiber, were clearly observed on the spectrum. The formation of these sidebands was a result of the constructive interference between the soliton pulses and dispersive waves, characteristic that the mode-locked pulses were optical solitons [24], [25]. The radio frequency (RF) signal to noise ratio was over 50 dB, which confirmed the stable mode-locking operation of the laser by using Fig. 5(c).

This article has been accepted for publication in a future issue of this journal, but has not been fully edited. Content may change prior to final publication. Citation information: DOI 10.1109/JPHOT.2015.2513199, IEEE Photonics Journal

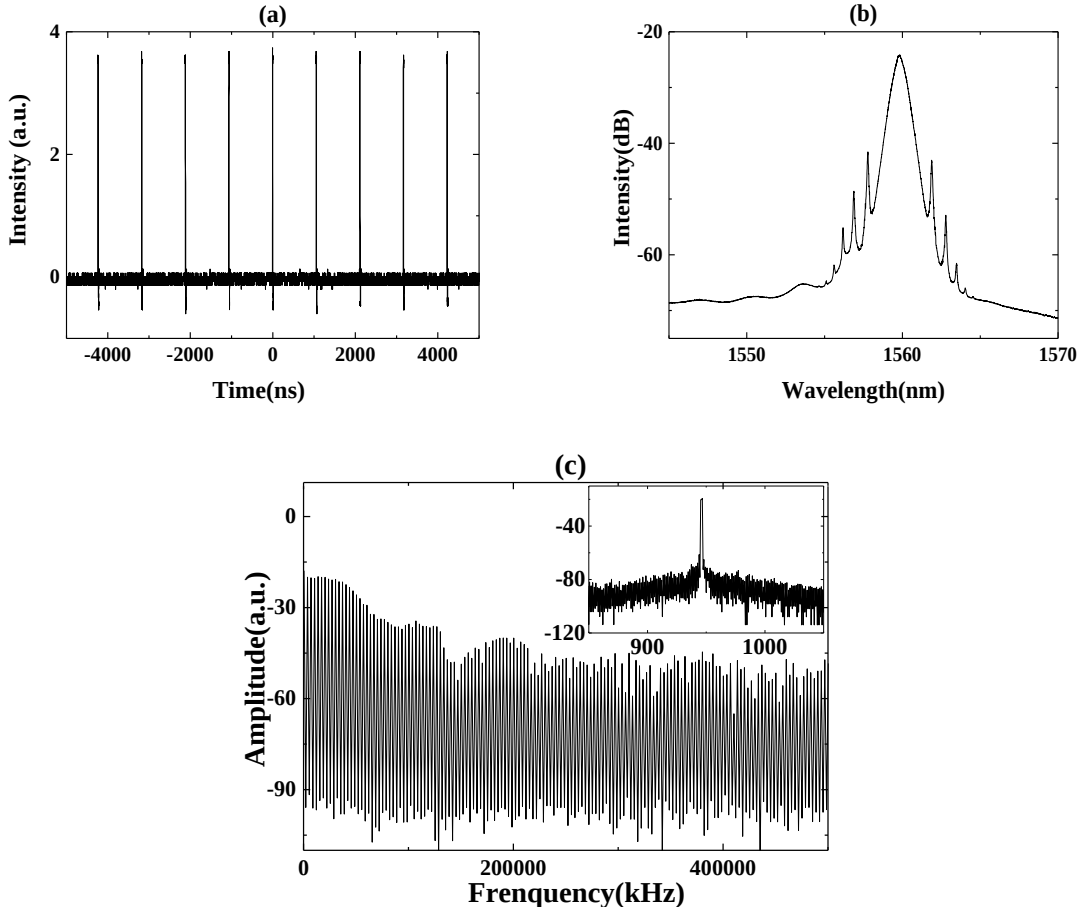

Fig. 5. (a) Mode-locked pulses; (b) The spectrum of the mode-locked pulses; (c) RF spectrum. Inset: RF spectrum around 940 kHz.

Particularly, a rectangular pulse profile was observed when you zoom into a single pulse, as shown in Fig. 6(a). As we know, a number of solitary wave solutions, such as flat-top solitons [26], [27], can be obtained from the extended complex Ginzburg–Landau equation. Moreover, a novel dissipative soliton resonance (DSR) effect is predicted with the selection of certain laser parameters [28]- [30]. Under DSR, the pulse width can increase indefinitely by increasing the pump power while keeping their amplitude constant. Fig. 6(b) shows that the pulse duration varied from 8.5 ns to 11.5 ns as the pump power is increased from 72 mW to 100 mW and the amplitude keeps constant, which indicates that our fiber laser operates in the DSR region. The pump powers of the red, blue, and black lines are 72 mW, 80 mW, and 100 mW, respectively. The inset in Fig. 6(b) shows the measured pulse width versus the pump power. When the pump power is above 150 mW, the MFG device will burn out because of the low damage threshold of the PMMA.

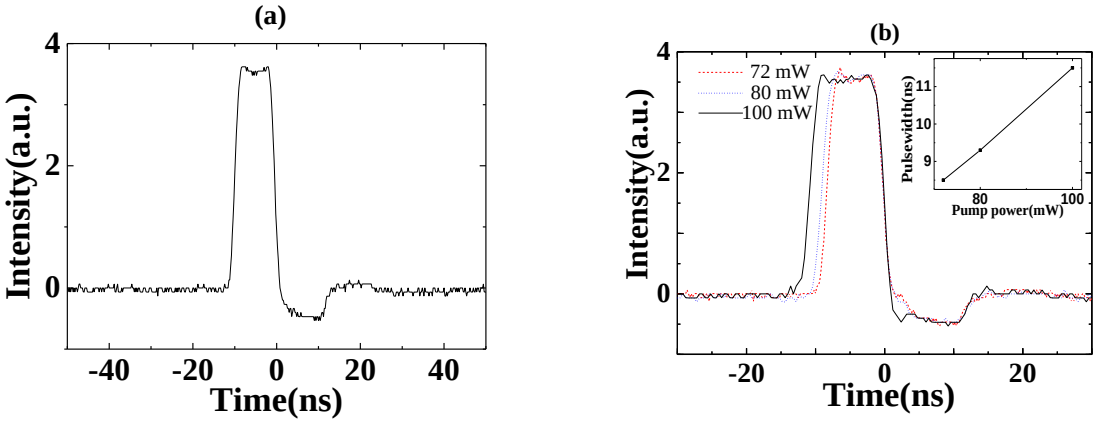

Fig. 6. (a) A single pulse when the pump power was 72 mW; (b) Pulse broadening when the pump power increased from 72 mW to 100 mW. The pump powers of the red, blue, and black line are 72 mW, 80 mW, and 100 mW, respectively. Inset: measured pulse width versus the pump power.

5. Conclusions

In this paper, we demonstrate a state variable erbium-doped fiber laser by using a MFG device. In order to enhance the NRP effect, a ~200 m SMF was added in the cavity. Stable Q-switched and mode-locked pulses can be obtained using a fixed pump power. In addition, the rectangular pulses are observed in our EDFL. The rectangular pulses have a pulse width and repetition rate of ~10 ns and ~940 kHz, respectively, and the Q-switched pulses have a pulse width and repetition rate of ~40 μs and ~4.8 kHz, respectively. To our knowledge, this is the first demonstration to achieve switching between rectangular pulses and Q-switched pulses while keeping the pump power constant by using a graphene SA. In the future, a compact fiber laser that can switch between nanosecond pulse and picosecond/femtosecond pulse is possible to be realized by optimizing the cavity and improving the transferring and cleaning process of the MFG device.

Acknowledgements

This study was supported by National 973 program (2011CBA00205), and National Natural Science Foundation of China (61322503, 61535005, 61475069).

References

[1] M. E. Fermann, and I. Hartl, “Ultrafast fibre lasers,” Nat. Photon., vol. 7, no. 11, pp. 868-874, 2013.

[2] F. W. Wise, A. Chong, and W. H. Renninger, “High-energy femtosecond fiber lasers based on pulse propagation at normal dispersion,” Laser. Photonics Rev., vol. 2, no. 1-2, pp. 58-73, 2008.

[3] S. D. Jackson, “Towards high-power mid-infrared emission from a fibre laser,” *Nat. Photon.,* vol. 6, no. 7, pp. 423-431, 2012.

[4] U. Keller, K. J. Weingarten, F. X. Kartner, D. Kopf, B. Braun, I. D. Jung, R. Fluck, C. Honninger, N. Matuschek, and J. Aus der Au, “Semiconductor saturable absorber mirrors (SESAM's) for femtosecond to nanosecond pulse generation in solid-state lasers,” *IEEE J. Sel. Topics Quantum Electron.,* vol. 2, no. 3, pp. 435-453, 1996.

[5] O. Oleg, G. Anatoly, and P. Markus, “Ultra-fast fibre laser systems based on SESAM technology: new horizons and applications,” *New J. Phys.,* vol. 6, no. 1, p. 177, 2004.

[6] L. Wang, X. Liu, Y. Gong, D. Mao, and L. Duan, “Observations of four types of pulses

in a fiber laser with large net-normal dispersion," *Opt. Express,* vol. 19, no. 8, pp. 7616-7624, 2011.

[7] M. Salhi, H. Leblond, and F. Sanchez, "Theoretical study of the erbium-doped fiber laser passively mode-locked by nonlinear polarization rotation," *Phys. Rev. A,* vol. 67, no. 1, p. 013802, 2003.

[8] F. X. Kurtner, J. A. der Au, and U. Keller, "Mode-locking with slow and fast saturable absorbers-what's the difference?," *IEEE J. Sel. Top. Quant. Electron.,* vol. 4, no. 2, pp. 159-168, 1998.

[9] H. A. Haus, "Mode-locking of lasers," *IEEE J. Sel. Top. Quant. Electron.,* vol. 6, no. 6, pp. 1173-1185, 2000.

[10] A. S. Kurkov, "Q-switched all-fiber lasers with saturable absorbers," *Laser Phys. Lett.,* vol. 8, no. 5, pp. 335-342, 2011.

[11] Z. Sun, T. Hasan, F. Torrisi, D. Popa, G. Privitera, F. Wang, F. Bonaccorso, D. M. Basko, and A. C. Ferrari, "Graphene Mode-Locked Ultrafast Laser," *ACS Nano,* vol. 4, no. 2, pp. 803-810, 2010.

[12] F. Bonaccorso, Z. Sun, T. Hasan, and A. C. Ferrari, "Graphene photonics and optoelectronics," *Nat. Photon.,* vol. 4, no. 9, p. 611-622, 2010.

[13] B. Fu, Y. Hua, X. S. Xiao, H. W Zhu, Z. P. Sun, and C. X. Yang, "Broadband Graphene Saturable Absorber for Pulsed Fiber Lasers at 1, 1.5, and 2 μm," *IEEE J. Sel. Top. Quant. Electron.,* vol. 20, no. 5, pp. 411-415, 2014.

[14] J. Lee, J. Koo, P. Debnath, Y. W. Song, and J. H. Lee, "A Q -switched, mode-locked fiber laser using a graphene oxide-based polarization sensitive saturable absorber," *Laser Phys. Lett.,* vol. 10, no. 3, p. 035103, 2013.

[15] N. Zhao, M. Liu, H. Liu, X. W. Zheng, Q. Y. Ning, A. P. Luo, Z. C. Luo, and W. C. Xu, "Dual-wavelength rectangular pulse Yb-doped fiber laser using a microfiber-based graphene saturable absorber," *Opt. Express,* vol. 22, no. 9, pp. 10906-10913, 2014.

[16] J. L. Kou, J. H. Chen, Y. Chen, F. Xu, and Y. Q. Lu, "Platform for enhanced light-graphene interaction length and miniaturizing fiber stereo devices," *Optica,* vol. 1, no. 5, pp. 307-310, 2014.

[17] Z. Zhang, C. Mou, Z. Yan, Y. Wang, K. Zhou, and L. Zhang, "Switchable dual-wavelength Q-switched and mode-locked fiber lasers using a large-angle tilted fiber grating," *Opt. Express,* vol. 23, no. 2, pp. 1353-1360, 2015.

[18] A. Hideur, T. Chartier, M. Brunel, M. Salhi, C. Özkul, and F. Sanchez, "Mode-lock, Q-switch and CW operation of an Yb-doped double-clad fiber ring laser," *Opt. Commun.,* vol. 198, no. 1–3, pp. 141-146, 2001.

[19] K. H. Lin, J. J. Kang, H. H. Wu, C. K. Lee, and G. R. Lin, "Manipulation of operation states by polarization control in an erbium-doped fiber laser with a hybrid saturable absorber," *Opt. Express,* vol. 17, no. 6, pp. 4806-4814, 2009.

[20] F. Xu and G. Brambilla, "Manufacture of 3-D Microfiber Coil Resonators," *IEEE Photon. Technol. Lett.,* vol. 19, no. 19, pp. 1481-1483, 2007.

[21] L. E. Nelson, D. J. Jones, K. Tamura, H. A. Haus, and E. P. Ippen, "Ultrashort-pulse fiber ring lasers," *Appl. Phys. B,* vol. 65, no. 2, pp. 277-294, 1997.

[22] H. Xu, D. Lei, S. Wen, X. Fu, J. Zhang, Y. Shao, L. Zhang, H. Zhang, and D. Fan, "Observation of central wavelength dynamics in erbium-doped fiber ring laser," *Opt. Express,* vol. 16, no. 10, pp. 7169-7174, 2008.

[23] J. Wu, D. Y. Tang, L. M. Zhao, and C. C. Chan, “Soliton polarization dynamics in fiber lasers passively mode-locked by the nonlinear polarization rotation technique,” *Phys. Rev. E,* vol. 74, no. 4, p. 046605, 2006.

[24] S. M. J. Kelly, “Characteristic sideband instability of periodically amplified average soliton,” *Electron. Lett.,* vol. 28, no. 8, pp. 806-807, 1992.

[25] L. Yung-Hsiang, and L. Gong-Ru, “Kelly sideband variation and self four-wave-mixing in femtosecond fiber soliton laser mode-locked by multiple exfoliated graphite nano-particles,” *Laser Phys. Lett,* vol. 10, no. 4, p. 045109, 2013.

[26] X. Li, X. Liu, X. Hu, L. Wang, H. Lu, Y. Wang, and W. Zhao, “Long-cavity passively mode-locked fiber ring laser with high-energy rectangular-shape pulses in anomalous dispersion regime,” *Opt. Lett.,* vol. 35, no. 19, pp. 3249-3251, 2010.

[27] X. L. Li, Z. S. M. Zhang, H. X. Zhang, M. M. Han, F. Wen, and Z. J. Yang, “Highly Efficient Rectangular Pulse Emission in a Mode-Locked Fiber Laser,” *IEEE Photon. Technol. Lett.,* vol. 26, no. 20, pp. 2082-2085, 2014.

[28] W. Chang, J. M. Soto-Crespo, A. Ankiewicz, and N. Akhmediev, “Dissipative soliton resonances in the anomalous dispersion regime,” *Phys. Rev. A,* vol. 79, no. 3, p. 033840, 2009.

[29] Z. C. Luo, W. J. Cao, Z. B. Lin, Z. R. Cai, A. P. Luo, and W. C. Xu, “Pulse dynamics of dissipative soliton resonance with large duration-tuning range in a fiber ring laser,” *Opt. Lett,* vol. 37, no. 22, pp. 4777-4779, 2012.

[30] X. Wu, D. Y. Tang, H. Zhang, and L. M. Zhao, “Dissipative soliton resonance in an all-normal-dispersion erbium-doped fiber laser,” *Opt. Express,* vol. 17, no. 7, pp. 5580-5584, 2009.